ZIBELINE INTERNATIONAL™ PUBLISHING

ISSN: 2576-6724 (Print)
ISSN: 2576-6732 (Online)
CODEN: ACMCCG

Acta Chemica Malaysia (ACMY)

DOI: http://doi.org/10.26480/acmy.01.2026.32.40

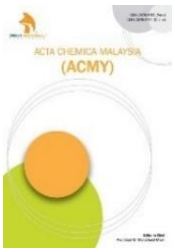

RESEARCH ARTICLE

RSM-OPTIMIZATION OF BIO-FUEL YIELD FROM FLUID CATALYTIC CRACKING OF COCONUT SHELL PYROLYTIC OIL WITH VACUUM GAS OIL

Tochukwu K. T, Ezeugo J. O, Umeuzuegbu J. C, Ndive J. N, Ojike P. C, Ifediorah E. I*

Department of Chemical Engineering, Chukwuemeka Odumegwu Ojukwu University, P.M.B. 6059. Anambra state, Nigeria.
Corresponding Author Email: ezekielifediorah@gmail.com

ARTICLE DETAILS

Article History:

Received 21 January 2026
Revised 27 January 2026
Accepted 12 February 2026
Available online 28 February 2026

ABSTRACT

This study optimizes the co-processing of coconut shell oil with vacuum gas oil (VGO) via fluid catalytic cracking (FCC) using response surface methodology (RSM). Coconut shells were characterized for its proximate, calorific value (HHV) and ultimate composition. The pyrolysis oil was produced from waste coconut shells via fast pyrolysis and characterised using Gas Chromatography-Mass Spectrometry (GC-MS) and Fourier Transform Infrared Spectroscopy (FTIR). The physicochemical properties of the pyrolysed oil, including viscosity, acid value, saponification value, specific gravity, ester value, and pH, were determined. The oil was cracked with vacuum gas oil using the fluid catalytic cracking process to produce the biofuel, which was further characterised using Fourier Transform Infrared Spectroscopy (FTIR). (RSM) Techniques were used to develop and optimise pyrolysis oil and biofuel yields among the considered factors (particle size, heating temperature, holding time, and reaction temperature) and (temperature, time, reactor riser, and dosage mixture), respectively. The proximate, calorific value (HHV) and ultimate analysis of the coconut shell, was determined as follows: moisture content 7.67%, volatile matter 66.1%, ash 1.4%, fixed carbon 24.8%, HHV 4339.85 kcal/kg, carbon 56.43%, hydrogen 4.16%, oxygen 37.51%, and nitrogen 0.48%. The pyrolysed oil shows a viscosity of 12.7 cP, a saponification value of 332.39 mg KOH/g, an ester value of 192.14 mg KOH/g, and an acid value of 140.25 mg KOH/g, demonstrating suitability but a high oxygenate content. The experimental and predicted yields for bio-oil was obtained at 62.35 and 64.12 wt% (particle size 1.5 mm, heating temp. 500 °C, holding time 60 min, reaction temp 550 °C) and for bio-fuel was obtained at 70.12 and 71wt%, under the operating parameters of temperature (500, 532°C), time (300, 228 min), reactor riser (30, 38 inches) and dosage mixture (0.5, 0.78). Quadratic models demonstrated excellent fit. The coefficient of determination (R2) for the pyrolysed oil and biofuel yields is 0.9914 and 0.9876, respectively. The quality of the model was investigated by analysis of variance (ANOVA).

KEYWORDS

coconut shell bio-oil, vacuum gas oil, fluid catalytic cracking, response surface methodology, Box-Behnken design, drop-in biofuel, zeolite catalyst

1. INTRODUCTION

The global shift to sustainable, low-carbon energy systems is rising amid increasing greenhouse gas emissions and fossil fuel depletion, with the transportation industry accounting for over 25% of energy-related CO_2 emissions. In 2017–2018, the transport sector accounted for 32% of global final energy consumption (TFEC), and 96.7% of these energy needs were met by fossil fuels. In 2019, the transport sector accounted for almost one-quarter of global energy-related greenhouse gas emissions (Kaltschmitt, 2019; Kumar and Verma, 2020; Hu and Gholizadeh, 2019). These growing concerns and environmental problems have prompted researchers and governments to seek cost-effective alternative fuel sources to conventional ones (González and Sandoval, 2020; Hu and Gholizadeh, 2019). Biomass-sourced liquid biofuels can be suitable alternative to fossil fuels. In recent years, biodiesel use has been increasing because of its advantages, such as affordability, renewability, cleanliness, and reduced pollution (Akbarian et al., 2022; Azhar et al., 2019). Its use is safe for the environment and for vehicular engines due to its physicochemical properties, which are similar to those of petroleum diesel. The global biodiesel market is projected to grow at a compound annual growth rate (CAGR) of 4.57% during 2017–2021. Biofuels from lignocellulosic biomass offer a renewable alternative, potentially reducing lifecycle emissions by 60-90% compared to petroleum-derived fuels (Bakar et al., 2020; Beims et al., 2020; Beydoun and Klankermayer, 2020). Coconut shell is promising due to its high lignin content (35-45 wt%) and low ash (<1 wt%), yielding aromatic-rich bio-oil via fast pyrolysis. However, crude bio-oil exhibits high oxygen content (30-0 wt%), high acidity (acid value 120–150 mg KOH/g), high viscosity, and thermal instability, which prevent direct use as transportation fuel and limit its integration into existing refineries (Bakar et al., 2020). Fluid catalytic cracking (FCC) co-processing with vacuum gas oil (VGO), a heavy petroleum fraction, is a cost-effective strategy for converting bio-oil oxygenates into gasoline- and diesel-range hydrocarbons (Ahamed et al., 2021; Bhatia et al., 2021; Draper et al., 2022). High bio-oil blending ratios typically lead to excessive coke formation, catalyst deactivation, and reduced liquid yields due to strong interactions among process variables such as temperature, residence time, riser geometry, and feed composition (Farooq et al., 2021; García Martín et al., 2020; Ge et al., 2022; Ghenai, Alamara, and Inayat, 2019; Ghenai, Inayat, Shanableh, et al., 2019). As synthesized bio-oil with Simulated fuel oil containing a mixture of ethyl (11.2%), butyl (10.6%) and isoamyl

Quick Response Code	Access this article online	
	Website: www.actachemicamalaysia.com	DOI: 10.26480/acmy.01.2026.3240

alcohols (78.2%) was used to obtain oil esters from palm kernel oil by enzymatic route employing lipase from *Burkholderia cepacia* immobilized on epoxy matrix silica-hydroxyethyl cellulose as a biocatalyst Runs were performed in both batch and continuous modes to determine the influence of the oil-to-alcohol molar ratio on ester concentrations, using isoamyl alcohol as the acyl acceptor (Siddique et al., 2025). The optimum oil to alcohol molar ratio was 1:4 and high isoamyl esters formation (99 wt%) was attained in 48 h (batch runs) and 8 h of space-time (continuous runs). Such conditions were used to perform transesterification reactions on palm kernel oil, yielding results similar to those obtained with simulated fossil oil rendering. The viscosity (kinematic at 40 °C) confirmed the high conversion by modifying the initial palm kernel oil viscosity from 30.13 $mm^2 s^{-1}$ to values ranging from 3 to 6 $mm^2 s^{-1}$. The viscosity index was 149.22 ± 2.11 and the oxidative stability was 23.85 ± 1.65 min. Also, the biocatalyst was found to be stable, with a half-life time ($t_{1/2}$) of about 38 days.

This research addresses a critical gap in the literature by focusing on the formulation and optimisation of biofuel from co-processed pyrolysed coconut shell oil with VGO. The comprehensive review confirms that significant research exists across the three domains relevant to this paper. One-factor-at-a-time experiments fail to capture the significant interactions among operating parameters. Response Surface Methodology (RSM) combined with Central Composite Design (CCD) is a powerful statistical tool that effectively models these interactions, predicts optimal conditions, and maximises desired responses with minimal experimental runs (Ifediorah, Babayemi, Eluno, and Eluno, 2025; Ifediorah and Ezeugo, 2025; Siddique et al., 2025). Coconut shell pyrolysis reliably produces bio-oil, but it is chemically inferior, characterized by high acidity and a dominant fraction of phenolic oxygenates. Co-processing bio-oil with petroleum fractions, such as VGO, is the necessary and preferred pathway for commercial adoption. While these individual components are established, a significant research gap exists in the integration of VGO, systematic optimization and modelling of the entire co-processing system: Lack of Integrated Optimization with VGO: Few studies have focused specifically on the catalytic co-processing of coconut husk bio-oil (with its unique, high-phenolic profile) using a single-step reactor system to maximize fuel quality (HHV) and minimize oxygen content simultaneously. There is a critical need to develop and validate high-predictive models using RSM to accurately capture the complex, non-linear synergistic interactions among the VGO/bio-oil ratio, temperature, and catalyst activity within the co-processing environment.

Therefore, the objective of this paper is to address this gap by establishing the optimal operating parameters and developing a highly dependable predictive model for the catalytic co-processing of coconut husk bio-oil with VGO to produce a refinery-ready, low-carbon liquid fuel.

The findings provide mathematical models for integrating coconut shell-derived bio-oil into existing petroleum refineries.

2. Materials and Methods

2.1 Materials

Coconut shells were acquired from waste dumps in Onitsha and Nnewi local markets in Anambra State. Sieves of various sizes, a Scrapper, a Jaw crusher, a Roller crusher, and a Davison Circulating Riser (DCR) setup were used in the research. Analytical-grade chemicals and distilled water were used.

2.2 Experimental methods

2.2.1 Preparation of coconut shells

A large number of coconut shells were collected from markets in Onitsha and Nnewi, Anambra State, Nigeria. The coconuts were initially sun-dried to minimise moisture content (especially the non-edible coconuts). The coconut shells collected were further dried for two days for further removal of moisture and the pulps surrounding the coconut shells were scooped with scrapper as shown in figure 1, to ensure particle removal and coconut shells fibre were removed by filing with a filler to obtain a smooth surface and a slight sheen to the shell. The sheen coconut shell was washed with distilled water and cut into smaller pieces and dried in an oven at 110^{o}C for an hour. (Ifediorah, Babayemi, Eluno, and Eluno, 2025; Ifediorah and Ezeugo, 2025; Ifediorah, Mmonwuba, Okolie, Toochukwu, and Ezeugo, 2025; Ifediorah and Ezeugo, 2024; Ifediorah, Akinpelu, Eluno, and Eluno, 2025). The dried sample's calorific value (HHV) and proximate and ultimate composition were determined below.

I. Proximate analysis

a. Moisture Content

As per ASTM D-3173, the moisture content of the raw biomass was determined by measuring the weight loss of the material in a hot-air oven. Subsequently, the moisture content was computed by using.

formula:

$$\text{Moisture, \% (wet basis)} = \frac{(W2 - W3)}{(W2 - W1)} \times 100 \quad (1)$$

$$\text{Moisture, \% (dry basis)} = \frac{(W2 - W3)}{(W3 - W1)} \times 100 \quad (2)$$

Were,

W1 = Weight of crucible, g

W2 = Weight of crucible + initial weight of sample, g

W3 = Weight of crucible + weight of dried sample, g

b. Volatile Matter

As per ASTM D-3175, the volatile matter was assessed by placing the oven-dried sample, obtained after determining the moisture content, in a sealed crucible at 950 ± 20 °C for 7 minutes in a muffle furnace (Quality NSW-101, MF-1, Temperature range 0-1200 °C). The weight loss was then measured as the percentage of volatile matter present in the sample.

$$\text{Volatile Matter, \% (dry basis)} = \frac{(W3 - W4)}{(W2 - W1)} \times 100 \quad (3)$$

Were,

W1 = Weight of crucible, g

W2 = Weight of crucible + sample, g

W3 = Weight of crucible +weight of sample before keeping in muffle furnace, g

W4 = Weight of crucible + weight of sample after keeping in muffle furnace, g

c. Ash Content

As per ASTM D-3174, the residual samples were heated gradually in a muffle furnace to 750 °C for 30 minutes. After cooling, they were weighed repeatedly until a constant weight was achieved. The weight of the residue indicated the sample ash content as a percentage basis.

$$\text{Ash, \% (dry basis)} = \frac{(W5 - W1)}{(W2 - W1)} \times 100 \quad (4)$$

Were,

W1 = Weight of crucible, g

W2 = Weight of crucible + sample, g

W5 = Weight of crucible + Constant weight of sample after

keeping in muffle furnace, g

d. Fixed Carbon

The fixed carbon (FC) content in the sample gives a rough indication of the charcoal yield. The fixed carbon is estimated by using the following formula.

Fixed carbon (%) = 100 - % of (moisture content + volatile matter + ash)

(5)

II. Heating Value of Coconut shell

The gross heating value of coconut shell (Cocos nucifera) was determined using a bomb calorimeter (ASTM E711) under controlled conditions at 25 atm of oxygen to ensure complete combustion. The water equivalent of the apparatus was determined by burning a known weight (1.0 g) of pure, dry benzoic acid in powdered form in the bomb under identical conditions, noting the rise in temperature for 5 minutes. The standard heating value of benzoic acid (6324 cal/g) was used to calculate the water equivalent. This allowed for the determination of the higher calorific value of coconut shell (Cocos nucifera) through the bomb calorimeter experiment was determined as:

Gross Calorific Value, $Q = \frac{[(W+w)(T2 - T1 + tC)] - [tA + tF + tT]}{m}$ (6)

Were,

W = Mass of water placed in the calorimeter, g

w = Water equivalent of the apparatus, g

T1 = Initial temperature of water in the calorimeter, °C

T2 = Final temperature of water in the calorimeter, °C

tC = Cooling correction

tA = Acid correction

tF = Fuse wire correction

tT = Cotton thread correction

m = Mass of fuel sample taken in the crucible, g

III. Ultimate Analysis

The ultimate analysis includes determining the carbon, hydrogen, oxygen, and nitrogen contents of the fuels. The ultimate analysis helps calculate heat balances in any process that uses biomass as fuel. Using the values from the proximate analysis, the ultimate analysis of the biomass was calculated using multilinear regression (MLR) equations to predict the elemental composition of coconut shell (Cocos nucifera) (Lawal et al., 2021).

a. Carbon Content, (%)

Carbon content (C) of the sample was calculated based on the following formula,

$C = 348.4658 - 2.36909FC - 2.97122VM - 3.5354A - 3.67567M$ (7)

b. Hydrogen Content, (%)

The hydrogen (H) content of the sample was calculated theoretically based on following formula,

$H = -6156.21 + 61.44348FC + 61.66506VM + 61.74225A + 61.65247M$ (8)

c. Oxygen Content, (%)

The oxygen (O) content of the sample was calculated theoretically by using the following formula,

$O = 31071.47 - 309.621FC - 310.437VM - 312.201A - 310.789M$ (9)

d. Nitrogen content, (%)

Nitrogen content (N) of the sample was theoretically calculated by difference using the following formula,

N = 100 - % of (C + H + O + Ash), % (10)

Were,

FC = Fixed Carbon, %

A = Ash content, %

VM = Volatile matter, %

M = Moisture content, %

2025).

Figure 1: Crushed coconut shells

2.2.2 Bio-oil extraction

The prepared sample (powdered coconut at different particle sizes) was fed directly into the fixed-bed reactor. Instead of air, Nitrogen gas was fed to the vertical reactor (furnace attached to the reactor) at 200ml/min rate). The use of Nitrogen was to control the heating value and the pyrolysis temperature to match with the conditions of the design of experiment conducted. Fast pyrolysis is an anaerobic process; hence, Nitrogen gas was used instead of air, which contains oxygen. The steam formed in the reactor during pyrolysis was collected in the bagasse, which flows together with the nitrogen at the top of the reactor. The gases were cooled using a water-filled condenser, and the temperature dropped from the design temperature to 50oC, turning the vapour phase into the liquid phase. The liquid product from the condenser was collected and the non-condensable gas was collected in a gas bag (James, Veethil, and Rajarathinam, 2022; Jaswal, Shende, Nan, Amar, and Shende, 2019; Jatoi et al., 2023; Johnston et al., 2019; Kaltschmitt, 2019; Kim, Tsang, Kwon, Lin, and Lee, 2019; Kumar and Verma, 2020).

The liquid product which was the bio-oil was stored in a cooling unit (refrigerator) and subjected to gas chromatograph mass spectroscopy (GC-MS) (GC-MS: Perkin Elmer Clarus 680 MS Clarus SQ 8T) and Fourier Transform Infrared Spectroscopy (FTIR). Table 1 shows the RSM experimental design data of pyrolytic oil.

Table 1: RSM Experimental design data of pyrolytic oil

Std	Runs	X1	X2	X3	X4
6	1	600	3		0.5
19	2	500	2		0.75
1	3	400	3		0.5
2	4	600	3		0.5
3	5	400	5		0.5
15	6	400	5	30	1
9	7	400	3	30	1
8	8	600	5	20	0.5
20	9	500	6	20	0.75
4	10	600	5	40	0.5
23	11	500	4	30	0.25
17	12	300	4	40	0.75
11	13	400	5	40	1
12	14	600	5	40	1
14	15	600	3	40	1
30	16	500	4	30	0.75
7	17	400	5	30	0.5
5	18	400	3	20	0.5
16	19	600	5	30	1
13	20	400	3	30	1
26	21	500	4	10	0.75
24	22	500	4	30	1.25
10	23	600	3	30	1
27	24	500	4	30	0.75
29	25	500	4	50	0.75
21	26	500	4		0.75
18	27	700	4		0.75
28	28	500	4		0.75
25	29	500	4		0.75
22	30	500	4		0.75

2.2.3 Co-processing of bio-oil and vacuum gas oil (VGO)

Using a Davison Circulating Riser (DCR) setup, the VGO was first heated to 50 °C to reduce viscosity and improve sample dispersion. The VGO was mixed with the bio-oil product and sent to the pre-heater. The pre-heater heated the feed to the run temperature, and the reactor temperature was also controlled to have the operating temperature equal to the inlet sample temperature. The inlet sample from the preheater was sent to the FCC reactor. The reactor temperature was maintained at the specified value for each run, and the holdup time was measured. The position of the reactor riser was set, and the reactor effluent was sent to the condensation tower, where cooling takes place to extract the liquid product, which was biodiesel. The top product was recycled back and mixed with the feed stream. The catalyst stripper removes the catalyst from the effluent, regenerating it, and the catalyst used was zeolite. The choice of zeolite catalyst stems from its ability to be regenerated by oxidation with air.

The biofuel was characterized using Fourier Transform Infrared Spectroscopy (FTIR) (Liu, Burra, Wang, Li, Che, and Gupta, 2021; Mathimani et al., 2019; Miranda, Motta, Maciel Filho, and Maciel, 2021;

Naushad, Sharma, and Alothman, 2019; Siddique, Ahmed, Aziz, et al., 2021; Siddique et al., 2025).

2.2.4 RSM modelling and Optimization process of the bio-oil and biofuel.

Using RSM, Interactive effects of process variables of reactor temperature (300-700°C), hold-up time in the reactor (120 min – 360 min), axial position of the reactor riser (10 – 60 in) and dosage mixture (bio-oil/VGO blend ratio) (0.25 – 1.25) on the bio-fuel yield was determined. The considered factors (particle size (mm), heating temp, holding time (min), and reaction temp) for bio-oil yield were investigated. Design Expert software version 13 was used to design the experiment. The process involves analysis of variance, mathematical modeling, graphical analyses, and validation of optimum results (Ifediorah et al., 2025; E.I. Ifediorah et al., 2025).

Multiple regression was used to estimate the polynomial model coefficients for the response variable to relate it to the independent factors. Analysis of variance (ANOVA) and a test of significance were used to assess the model's fit quality. The following equation describes the fitted quadratic response model [35].

$$y = a_0 + a_1x_1 + a_2x_2 + a_3x_3 + a_4x_4 + a_5x_1^2 + a_6x_2^2 + a_7x_3^2 + a_8x_4^2 \quad (1)$$

Where y represents the response, x_1 to x_4 represents the factors for each of the responses and a_0 to a_{14} represents the model coefficients.

3. Results and Discussions

3.1 Physicochemical properties of Bio-Oil

The produced bio-oil is a homogenous dark-brown liquids with no phase separation was observed upon storage. The physical properties of the bio-oil were determined and recorded in Table 2. The bio-oil had a high acid value, and its high moisture content significantly reduced viscosity.

Table 2: Physicochemical properties of bio-oil.

Parameters	values
Specific gravity (g/ml)	0.98
Acid value	330.23
Saponification value	189.41
Ester value	64.21
pH	2.90
Viscosity (cP)	13.98

3.2 Gas Chromatography-Mass Spectrometry of bio-oil

The coconut shell consists of lignocellulosic components, including hemicellulose, cellulose, and lignin. During thermal degradation, these components are converted into various types of hydrocarbons, carboxylic acids, acid derivatives, and phenols. The GC-MS chromatogram of the pyrolytic oil is shown (Figure 2) was analysed to determine the oil's exact composition of which phenol and phenol derivatives are the major (Ifediorah, Babayemi, Eluno, and Eluno, 2025; Ifediorah and Ezeugo, 2025; Ifediorah, Mmonwuba, Okolie, Toochukwu, and Ezeugo, 2025; Ifediorah and Ezeugo, 2024; Ifediorah, Akinpelu, Eluno, and Eluno, 2025).

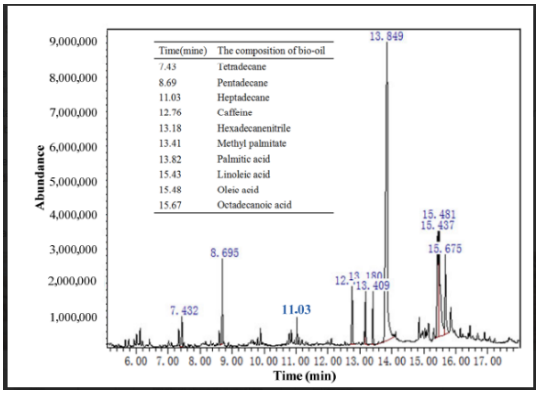

Figure 2: GC-MS spectra of the Bio-oil

3.3 Fourier Transform Infrared Spectroscopy of upgraded oil (biofuel)

FT-IR spectra of the upgraded bio-oil are presented in figure 3; From the FTIR analysis, the substantial attenuation of the O-H and general C-O stretching bands confirms the effective removal of highly polar and unstable oxygenates facilitated by the the VGO/ZSM. The presence of strong, dominant C-H stretching bands reveals the conversion of oxygenated species into stable, high-energy aliphatic hydrocarbons. Peak aromatic groups, further confirms the catalytic cracking and cyclization activity of the ZSM catalyst, producing desirable gasoline-range components (Farooq et al., 2021; García Martín et al., 2020).

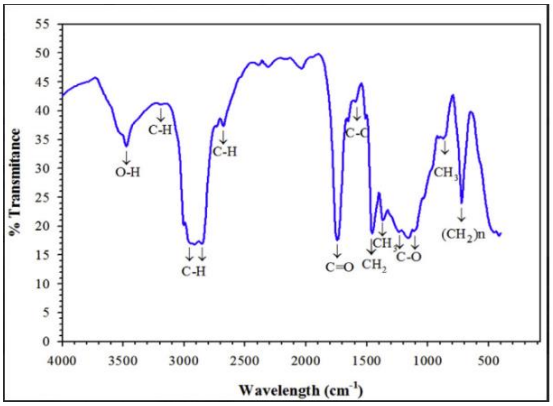

Figure 3: FT-IR spectrum of the Bio-oil

3.4 Model Fit Summary and Analysis of Variance (ANOVA) of the bio-oil and biofuel

Table 3 present the actual and RSM-predicted responses for bio-oil. It demonstrated how the Actual response interacted with the predicted response. To maximise the interactive effects of the process factors on yields, the best-suited model among the four examined was the quadratic model. Finding the quadratic model for the yields and its optimal reaction conditions involves analysing the ANOVA data. Equations 2 and 3 offer quadratic models of bio-oil and biofuel in terms of coded components (Draper et al., 2022; Farooq et al., 2021; Siddique et al., 2025).

$$y = 1.5244 - 0.033x_1 - 0.0389x_2 + 0.0181x_3 - 0.0006x_4 + 0.0013x_1x_2 + 0.0019x_1x_3 + 0.0011x_2x_3 - 0.0001x_3x_4 + 0.0001x_1^2 + 0.0048x_3^2 \quad (2)$$

$$y = 0.7529 + 0.0005x_1 + 0.1189x_2 - 0.0051x_3 - 0.292x_4 - 0.0002x_1x_2 - 0.0001x_1x_4 - 0.0002x_2x_3 + 0.0179x_2x_4 + 0.0039x_3x_4 - 0.0067x_2^2 + 0.1134x_4^2 \quad (3)$$

Table 3: Actual and RSM predicted responses of bio-oil yield.

Runs	Actual response	Quadratic prediction
1	0.9201	0.9178
2	0.9358	0.8688
3	0.8018	0.8175
4	0.9371	0.9272
5	0.8888	0.8670
6	0.7968	0.8257
7	0.8279	0.8549
8	0.8741	0.9105
9	0.9447	0.9571
10	0.9460	0.8885
11	0.8071	0.8688
12	0.9469	0.9040
13	0.9446	0.9554
14	0.8635	0.8770
15	0.9176	0.9088
16	0.8044	0.8688
17	0.8525	0.8688
18	0.9375	0.9228
19	0.9163	0.8688
20	0.9450	0.9608
21	0.8928	0.8496
22	0.7861	0.8209
23	0.9261	0.9441
24	0.9406	0.9592
25	0.8967	0.8688
26	0.9103	0.8794
27	0.9078	0.8938
28	0.8475	0.8380
29	0.8927	0.9053
30	0.8094	0.8203

3.5 ANOVA (analysis of variance) for quadratic model of bio-oil and bio-fuel yield

Table 4 present the ANOVA results for the quadratic model of bio-fuel yields. the model's F-values of 4.42 and 4.54 indicate that the models are significant. An F-value this large could only be the result of noise in 0.01% of cases. Model terms are considered significant when the P-value is less than 0.0500. The difference is less than 0.2 for bio-oil and 0.5 for biofuel, meaning that the adjusted R^2 for the bio-oil and biofueled 0.3177 and

0.4487, and their corresponding predicted R^2 of 0.5223 and 0.8237 are in reasonable agreement. Adequate precision quantifies the signal-to-noise ratio. A ratio greater than four is desirable. This model can be used to navigate the design space (Siddique et al., 2025).

Table 4: ANOVA for biofuel

coefficient	Square error	F-value	P-value	Statistical parameters
1.5244	0.3355	4.5437	0.0004	
-0.0330	0.0204	-1.6137	0.1274	
-0.0389	0.0163	-2.3790	0.0311	
0.0181	0.0817	0.2212	0.8279	
-0.0006	0.0004	-1.5044	0.1532	
0.0013	0.0006	2.2171	0.0425	
0.0019	0.0028	0.6641	0.5167	R^2= 0.8237
0.0000	0.0000	0.1736	0.8645	adjR^2=0.4487
0.0011	0.0023	0.4745	0.6420	mse= 0.000004
0.0000	0.0000	2.6933	0.0167	rmse= 0.0021
-0.0001	0.0001	-1.8909	0.0781	
0.0001	0.0005	0.2505	0.8056	
0.0000	0.0003	0.0831	0.9349	
0.0048	0.0087	0.5521	0.5890	
0.0000	0.0000	1.7817	0.0950	

3.6 Results validation and optimum RSM results of the pyrolytic oil and biofuel yield

The experimental and predicted yields for bio-oil was obtained at 62.35 and 64.12 wt% (particle size 1.5 mm, heating temp. 500 °C, holding time 60 min, reaction temp 550 °C) and for bio-fuel was obtained at 70.12 and 71wt%, under the operating parameters of temperature (500, 532°C), time (300, 228 min), reactor riser (30, 38 inches) and dosage mixture (0.5, 0.78). Using the percentage deviation method, the experimental and predicted bio-oil and bio-fuel yields were compared. The percentage deviation is below the 5% threshold. As a result, the developed model accurately predicted the experimental results. The 3D plots, Figures 4 and 5, presented the RSM graphical results. Each one shows a parabolic curve, typical of a quadratic model. Thus, the experimental data were effectively predicted by the generated RSM model (Draper et al., 2022; Farooq et al., 2021; Siddique et al., 2025).

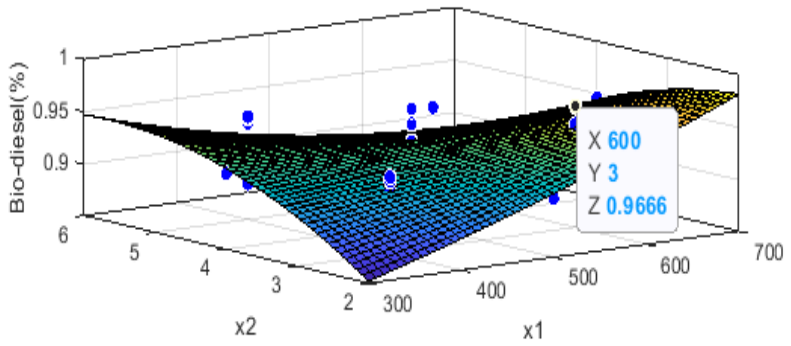

Figure 4: Surface and contour plot of the interaction of temperature and reactor hold up time on the response.

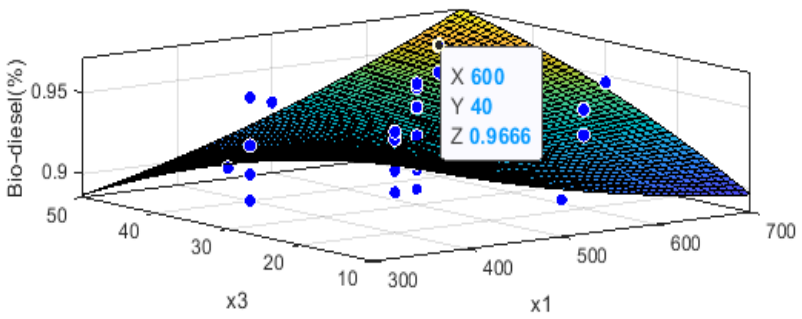

Figure 5: Surface and contour plot of the interaction of temperature and riser position on the response.

4. Conclusion

This study demonstrated a method for transforming waste coconut shells into high-grade, low-carbon biofuel through a two-stage process involving fast pyrolysis followed by fluid catalytic cracking (FCC) co-processing with vacuum gas oil (VGO). The physiochemical properties of bio-oil produced from fast pyrolysis of coconut shell shows high oxygen content, acid value (140.25 mg KOH/g), and viscosity of 12.7 cP. These poor properties necessitate catalytic upgrading for integration into the refinery. Response Surface Methodology (RSM) with Central Composite Design demonstrated

its effectiveness in optimizing both stages (Pyrolysis and FCC). For the pyrolysis stage, the quadratic model demonstrated an excellent fit (R^2 = 0.9914), achieving an optimal experimental bio-oil yield of 62.35 wt% and an optimised yield of 64.12 wt% at particle size of 1.5 mm, heating temperature of 500 °C, holding time of 60 min, and reaction temperature of 550 °C. In the biofuel, the quadratic model again showed strong predictive capability (R^2 = 0.9876), achieving an optimum experimental bio-fuel) yield of 70.12 wt% and optimized yield of 71.0 wt% under optimized conditions of 532 °C reactor temperature, 228 min (3.8 h) hold-up time, 38-inch riser axial position, and a bio-oil/VGO dosage ratio of 0.78. FTIR analysis of the upgraded biofuel revealed effective deoxygenation, with significant reductions in O–H and C=O bands and improvements in aliphatic and aromatic C–H stretching, indicating effective conversion to a stable hydrocarbon fuel. The close agreement between experimental and predicted values (percentage deviation < 5%) validates the accuracy and reliability of the developed RSM models.

REFERENCES

Abdurrahman, M. I., Chaki, S., and Saini, G., 2020. Stubble burning: Effects on health and environment, regulations, and management practices. Environmental Advances, 2, 100011. https://doi.org/10.1016/j.envadv.2020.100011

Ahamed, T. S., Anto, S., Mathimani, T., Brindhadevi, K., and Pugazhendhi, A., 2021. Upgrading of bio-oil from thermochemical conversion of various biomass—Mechanism, challenges, and opportunities. Fuel, 287, 119329. https://doi.org/10.1016/j.fuel.2020.119329

Ahmed, M. J., and Hameed, B. H., 2020. Insight into the co-pyrolysis of different blended feedstocks to biochar for the adsorption of organic and inorganic pollutants: A review. Journal of Cleaner Production, 265, 121762. https://doi.org/10.1016/j.jclepro.2020.121762

Akbarian, A., Andooz, A., Kowsari, E., Ramakrishna, S., Asgari, S., and Cheshmeh, Z. A., 2022. Challenges and opportunities of lignocellulosic biomass gasification on the path to the circular bioeconomy. Bioresource Technology, 362, 127774. https://doi.org/10.1016/j.biortech.2022.127774

Azhar, A., Yamauchi, Y., Allah, A. E., Alothman, Z. A., Badjah, A. Y., Naushad, M., Habila, M., Wabaidur, S., Wang, J., and Zakaria, M. B., 2019. Nanoporous iron oxide/carbon composites through in-situ deposition of prussian blue nanoparticles on graphene oxide nanosheets and subsequent thermal treatment for supercapacitor applications. Nanomaterials, 9(5), Pp. 776. https://doi.org/10.3390/nano9050776

Bakar, M. S. A., Ahmed, A., Jeffery, D. M., Hidayat, S., Sukri, R. S., Mahlia, T. M. I., Jamil, F., Khurrum, M. S., Inayat, A., Moogi, S., and Park, Y.-K., 2020. Pyrolysis of solid waste residues from lemon myrtle essential oils extraction for bio-oil production. Bioresource Technology, 318, 123913. https://doi.org/10.1016/j.biortech.2020.123913

Beims, R. F., Hu, Y., Shui, H., and Xu, C. C., 2020. Hydrothermal liquefaction of biomass to fuels and value-added chemicals: Products, applications, and challenges to develop large-scale operations. Biomass and Bioenergy, 135, 105510. https://doi.org/10.1016/j.biombioe.2020.105510

Beydoun, K., and Klankermayer, J., 2020. Efficient plastic waste recycling to value-added products by integrated biomass processing. ChemSusChem, 13(3), Pp. 488-492. https://doi.org/10.1002/cssc.201902880

Bhatia, S. K., Bhatia, R. K., Jeon, J.-M., Pugazhendhi, A., Awasthi, M. K., Kumar, D., Kumar, G., Yoon, J.-J., and Yang, Y.-H., 2021. An overview on advancements in biobased transesterification methods for biodiesel production: Oil resources, extraction, biocatalysts, and process intensification technologies. Fuel, 285, 119117. https://doi.org/10.1016/j.fuel.2020.119117

Cerón, A. A., Boas, R. N. V., Biaggio, F. C., and de Castro, H. F., 2018. Synthesis of biolubricant by transesterification of palm kernel oil with simulated fuel oil: Batch and continuous processes. Biomass and Bioenergy, 119, Pp. 166-172.

Draper, B., Yee, W. L., Pedrana, A., Kyi, K. P., Qureshi, H., Htay, H., Naing, W., Thompson, A. J., Hellard, M., and Howell, J., 2022. Reducing liver disease-related deaths in the Asia-Pacific: The important role of decentralised and non-specialist led hepatitis C treatment for cirrhotic patients. The Lancet Regional Health – Western Pacific, 20. https://doi.org/10.1016/j.lanwpc.2021.100359

Farooq, A., Moogi, S., Jang, S.-H., Ahmed, A., Kim, Y.-M., Kannapu, H. P. R., Valizadeh, S., Jung, S.-C., Lam, S. S., Rhee, G. H., and Park, Y.-K., 2021. Biohydrogen synthesis from catalytic steam gasification of furniture waste using nickel catalysts supported on modified CeO2. International Journal of Hydrogen Energy, 46(31), Pp. 16603-16611. https://doi.org/10.1016/j.ijhydene.2020.12.086

García Martín, J. F., Cuevas, M., Feng, C.-H., Álvarez Mateos, P., Torres Garcia, M., and Sánchez, S., 2020. Energetic valorisation of olive biomass: Olive-tree pruning, olive stones and pomaces. Processes, 8(5), Pp. 511. https://doi.org/10.3390/pr8050511

Ge, H., Zheng, J., and Xu, H., 2022. Advances in machine learning for high value-added applications of lignocellulosic biomass. Bioresource Technology. https://doi.org/10.1016/j.biortech.2022.128481

Ghenai, C., Alamara, K., and Inayat, A., 2019. Solar-assisted pyrolysis of plastic waste: Pyrolysis oil characterization and grid-tied solar PV power system design. Energy Procedia, 159, Pp. 123-129. https://doi.org/10.1016/j.egypro.2018.12.029

Ghenai, C., Inayat, A., Shanableh, A., Al-Sarairah, E., and Janajreh, I., 2019. Combustion and emissions analysis of spent pot lining (SPL) as alternative fuel in cement industry. Science of The Total Environment, 684, Pp. 519-526. https://doi.org/10.1016/j.scitotenv.2019.05.157

González, C. A. D., and Sandoval, L. P., 2020. Sustainability aspects of biomass gasification systems for small power generation. Renewable and Sustainable Energy Reviews, 134, 110180. https://doi.org/10.1016/j.rser.2020.110180

Hu, X., and Gholizadeh, M., 2019. Biomass pyrolysis: A review of the process development and challenges from initial research to the commercialisation stage. Journal of Energy Chemistry, 39, Pp. 109-143. https://doi.org/10.1016/j.jechem.2019.01.024

Ifediorah, E. I., and Ezeugo J. O. 2025. Environmental impact and optimization of bio-hydraulic fluid from biobased oil and friction modifiers (Eggshell and Snail shell). UNIZIK Journal of Engineering and Applied Sciences, 5(1), Pp. 2345–2363. https://journals.unizik.edu.ng/ujeas/article/view/6148

Ifediorah, E. I., Babayemi, A. K., Eluno, O. L., and Eluno, E. E., 2025. Experimental evaluation and RSM optimization of bio-grease from cottonseed oil using sodium hydroxide and bio-based additives. Journal of Engineering Research and Reports, 27(5), Pp. 463-481. https://doi.org/10.9734/jerr/2025/v27i51518

Ifediorah, E. I., Mmonwuba, N. C., Okolie, L. E., Toochukwu, K. T., and Ezeugo, J. O., 2025. Formulation and performance evaluation of sustainable bio-hydraulic fluid from spent palm kernel oil glycerin and Anacardium occidentale leaf extract as a corrosion inhibitor. Journal of Engineering Research and Reports, 27(5), Pp. 443-462. https://doi.org/10.9734/jerr/2025/v27i51517

Ifediorah, E., and Ezeugo, J., 2024, November 02. Acta Chemica Malaysia (ACMY). SSRN. https://ssrn.com/abstract=5319002 or http://dx.doi.org/10.2139/ssrn.5319002

Ifediorah, E., Akinpelu, B., Eluno, O. L., and Eluno, E. E., 2025. Development and evaluation of biogrease from biobased oil using palm bunch lye, and Moringa oleifera leaf. SSRN. https://ssrn.com/abstract=5268428 or http://dx.doi.org/10.2139/ssrn.5268428

James, J. J., Veethil, S. K., and Rajarathinam, J. R. J., 2022. Formulation and evaluation of topical preparations containing pyrolytic oil obtained from local biomass. Indian Journal of Pharmaceutical Education and Research, 56(2s), Pp. s163-s170. https://doi.org/10.5530/ijper.56.2s.87

Jaswal, R., Shende, A., Nan, W., Amar, V., and Shende, R., 2019. Hydrothermal liquefaction and photocatalytic reforming of pinewood (Pinus ponderosa)-derived acid hydrolysis residue for hydrogen and bio-oil production. Energy and Fuels, 33(7), Pp. 6454-6462. https://doi.org/10.1021/acs.energyfuels.9b01071

Jatoi, A. S., Ahmed, J., Akhter, F., Sultan, S. H., Chandio, G. S., Ahmed, S., Hashmi, Z., Usto, M. A., Shaikh, M. S., Siddique, M., and Maitlo, G., 2023. Recent advances and treatment of emerging contaminants through the bio-assisted method: A comprehensive review. Water, Air, and Soil Pollution, 234(1), 49. https://doi.org/10.1007/s11270-022-06037-2

Johnston, H. J., Mueller, W., Steinle, S., Vardoulakis, S., Tantrakarnapa, K., Loh, M., and Cherrie, J. W., 2019. How harmful is particulate matter emitted from biomass burning? A Thailand perspective. Current Pollution Reports, 5(4), Pp. 353-377. https://doi.org/10.1007/s40726-019-00125-4

Kaltschmitt, M. (Ed.)., 2019. Energy from Organic Materials (Biomass). Springer New York. https://doi.org/10.1007/978-1-4939-7813-7

Kim, S., Tsang, Y. F., Kwon, E. E., Lin, K.-Y. A., and Lee, J., 2019. Recently developed methods to enhance the stability of heterogeneous catalysts for conversion of biomass-derived feedstocks. Korean Journal of Chemical Engineering, 36, Pp. 1-11. https://doi.org/10.1007/s11814-018-0174-x

Kumar, B., and Verma, P., 2020. Biomass-based biorefineries: An important architype towards a circular economy. Fuel, 288, 119622. https://doi.org/10.1016/j.fuel.2020.119622

Liu, X., Burra, K. R. G., Wang, Z., Li, J., Che, D., and Gupta, A. K., 2021. Towards enhanced understanding of synergistic effects in co-pyrolysis of pinewood and polycarbonate. Applied Energy, 289, 116662. https://doi.org/10.1016/j.apenergy.2021.116662

Mathimani, T., Baldinelli, A., Rajendran, K., Prabakar, D., Matheswaran, M., van Leeuwen, R. P., and Pugazhendhi, A., 2019. Review on cultivation and thermochemical conversion of microalgae to fuels and chemicals: Process evaluation and knowledge gaps. Journal of Cleaner Production, 208, Pp. 1053-1064. https://doi.org/10.1016/j.jclepro.2018.10.096

Miranda, N. T., Motta, I. L., Maciel Filho, R., and Maciel, M. R. W., 2021. Sugarcane bagasse pyrolysis: A review of operating conditions and product properties. Renewable and Sustainable Energy Reviews, 149, 111394. https://doi.org/10.1016/j.rser.2021.111394

Naushad, M., Sharma, G., and Alothman, Z. A., 2019. Photodegradation of toxic dye using Gum Arabic-crosslinked-poly(acrylamide)/Ni(OH)2/FeOOH nanocomposites hydrogel. Journal of Cleaner Production, 241, 118263. https://api.semanticscholar.org/CorpusID:203314092

Siddique, M., Ahmed, S., Aziz, S., et al., 2021. An overview of recent advances and novel synthetic approaches for lignocellulosic derived biofuels. J Kejuruter., 33(2), Pp. 165-173. https://doi.org/10.17576/jkukm-2021-33(2)-01

Siddique, M., Wakeel, A., Asif, M., Laghari, M., and K., S., 2025. Optimization of Biodiesel Synthesis from Waste Cooking Oil Using a Heterogeneous Green Catalyst. Portugaliae Electrochimica Acta, 43(6), Pp. 395-401. https://doi.org/10.4152/pea.202.